

Received 11 March 2019

Accepted 28 March 2019

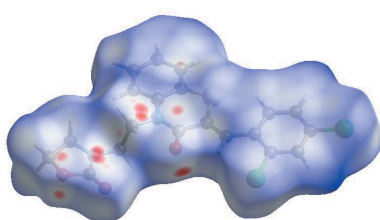
Edited by A. J. Lough, University of Toronto,
Canada**Keywords:** crystal structure; dihydrobenzothiazine; oxazole; π -stacking; Hirshfeld surface.**CCDC reference:** 1906476**Supporting information:** this article has supporting information at journals.iucr.org/e

Crystal structure, Hirshfeld surface analysis and DFT study of (2Z)-2-(2,4-dichlorobenzylidene)-4-[2-(2-oxo-1,3-oxazolidin-3-yl)ethyl]-3,4-dihydro-2H-1,4-benzothiazin-3-one

Brahim Hni,^{a*} Nada Kheira Sebbar,^{b,a} Tuncer Hökelek,^c Lhoussaine El Ghayati,^a Younes Bouzian,^a Joel T. Mague^d and El Mokhtar Essassi^{a,e}

^aLaboratoire de Chimie Organique Hétérocyclique URAC 21, Pôle de Compétence Pharmacochimie, Av. Ibn Battouta, BP 1014, Faculté des Sciences, Université Mohammed V, Rabat, Morocco, ^bLaboratoire de Chimie Bioorganique Appliquée, Faculté des sciences, Université Ibn Zohr, Agadir, Morocco, ^cDepartment of Physics, Hacettepe University, 06800 Beytepe, Ankara, Turkey, ^dDepartment of Chemistry, Tulane University, New Orleans, LA 70118, USA, and ^eMoroccan Foundation for Advanced Science, Innovation and Research (MASCIR), Rabat, Morocco. *Correspondence e-mail: brahimhni2018@gmail.com

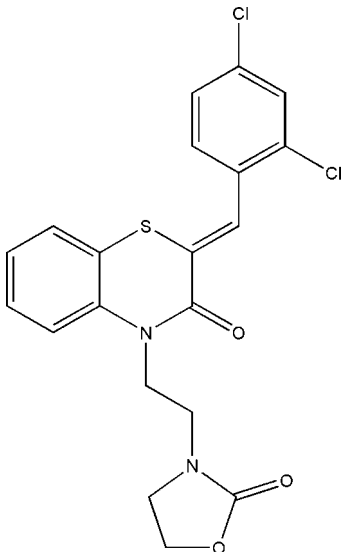
The title compound, $C_{20}H_{16}Cl_2N_2O_3S$, is built up from a dihydrobenzothiazine moiety linked by $-CH-$ and $-C_2H_4-$ units to 2,4-dichlorophenyl and 2-oxo-1,3-oxazolidine substituents, where the oxazole ring and the heterocyclic portion of the dihydrobenzothiazine unit adopt envelope and flattened-boat conformations, respectively. The 2-carbon link to the oxazole ring is nearly perpendicular to the mean plane of the dihydrobenzothiazine unit. In the crystal, the molecules form stacks extending along the normal to (104) with the aromatic rings from neighbouring stacks intercalating to form an overall layer structure. The Hirshfeld surface analysis of the crystal structure indicates that the most important contributions for the crystal packing are from $H \cdots H$ (28.4%), $H \cdots Cl/Cl \cdots H$ (19.3%), $H \cdots O/O \cdots H$ (17.0%), $H \cdots C/C \cdots H$ (14.5%) and $C \cdots C$ (8.2%) interactions. Weak hydrogen-bonding and van der Waals interactions are the dominant interactions in the crystal packing. Density functional theory (DFT) optimized structures at the B3LYP/ 6-311 G(d,p) level are compared with the experimentally determined molecular structure in the solid state. The HOMO–LUMO behaviour was elucidated to determine the energy gap.



1. Chemical context

Compounds containing a 1,4-benzothiazine backbone have been studied extensively both in academic and industrial laboratories. These molecules exhibit a wide range of biological applications indicating that the 1,4-benzothiazine moiety is a template potentially useful in medicinal chemistry research and therapeutic applications such as antipyretic (Warren & Knaus, 1987), anti-microbial (Armenise *et al.*, 2012; Rathore & Kumar, 2006; Sabatini *et al.*, 2008), anti-viral (Malagu *et al.*, 1998), herbicide (Takemoto *et al.*, 1994), anti-cancer (Gupta & Kumar, 1986) and anti-oxidant (Zia-ur-Rehman *et al.*, 2009) areas. They have also been reported as precursors for the syntheses of new compounds (Vidal *et al.*, 2006) possessing anti-diabetic (Tawada *et al.*, 1990) and anti-corrosion activities (Ellouz *et al.*, 2016*a,b*). 1,4-Benzothiazine-containing compounds are important because of their potential applications in the treatment of diabetes complications, by inhibiting aldose reductase (Aotsuka *et al.*, 1994). They are

also used as analgesics (Wammack *et al.*, 2002) and antagonists of Ca^{2+} (Fujimura *et al.*, 1996). As a continuation of our previous work on the syntheses and the biological properties of new 1,4-benzothiazine derivatives (Sebbar *et al.*, 2016*a,b*; Ellouz *et al.*, 2015*a,b*, 2017*a,b*), we report herein on the synthesis and the molecular and crystal structures of the title compound, (I), along with the Hirshfeld surface analysis and the density functional theory (DFT) calculations.



2. Structural commentary

The title compound, (I), is built up from a dihydrobenzothiazine moiety linked by $-\text{CH}-$ and C_2H_2- units to 2,4-dichlorophenyl and 2-oxo-1,3-oxazolidine substituents, respectively (Fig. 1). The benzene ring, *A* (*C*1–*C*6), is oriented at a dihedral angle of $11.27(6)^\circ$ with respect to the phenyl ring *D* (*C*15–*C*20), ring *A*. A puckering analysis of the heterocyclic

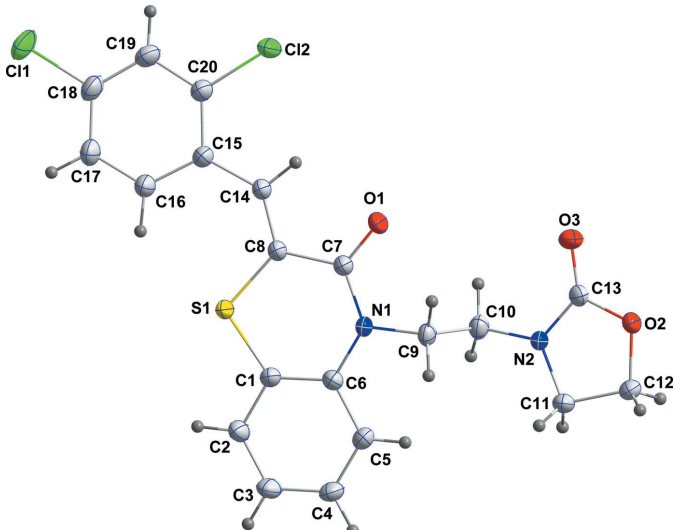


Figure 1

The molecular structure of the title compound with the atom-numbering scheme. Displacement ellipsoids are drawn at the 50% probability level.

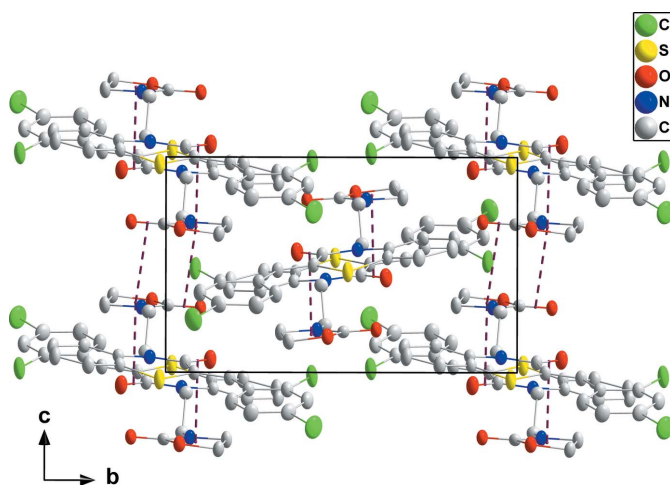


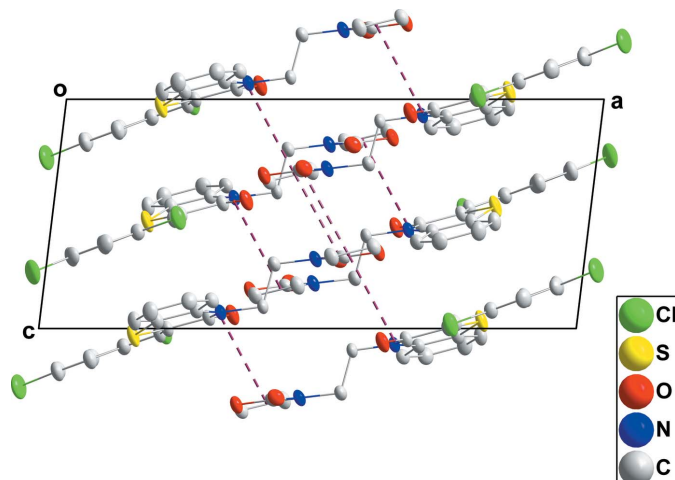
Figure 2

A partial packing diagram viewed along the *a*-axis direction with the π -stacking interactions shown by dashed lines.

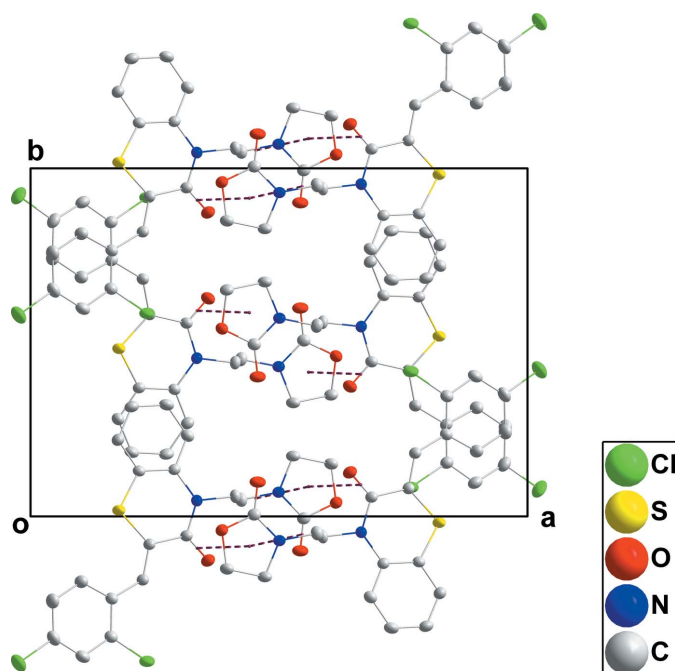
portion (ring *B*; *S*1/*N*1/*C*1/*C*6–*C*8) of the dihydrobenzothiazine unit gave the parameters $Q_T = 0.1206(14)$ Å, $q_2 = 0.1190(14)$ Å, $q_3 = -0.0174(16)$ Å, $\varphi = 178.2(8)^\circ$ and $\theta = 98.4(8)^\circ$, indicating a flattened-boat conformation. A similar analysis for the oxazolidine ring *C* (*O*2/*N*2/*C*11–*C*13) yielded $q_2 = 0.1125(18)$ Å and $\varphi_2 = 45.7(9)^\circ$, indicating an envelope conformation with atom *C*12 at the flap position and at a distance of $0.175(2)$ Å from the best plane of the other four atoms. The *C*9/*C*10 chain *C* is essentially perpendicular to the dihydrobenzothiazine unit, as indicated by the *C*6–*N*1–*C*9–*C*10 torsion angle of $90.61(19)^\circ$. In the heterocyclic ring *B*, the *C*1–*S*1–*C*8 [$104.29(8)^\circ$], *S*1–*C*8–*C*7 [$121.39(12)^\circ$], *C*8–*C*7–*N*1 [$120.77(14)^\circ$], *C*7–*N*1–*C*6 [$126.86(14)^\circ$], *C*6–*C*1–*S*1 [$123.97(13)^\circ$] and *N*1–*C*6–*C*1 [$121.60(15)^\circ$] bond angles are enlarged compared with the corresponding values in the closely related compounds (*2Z*)-2-(4-chlorobenzylidene)-4-[2-(2-oxooxazoliden-3-yl)ethyl]-3,4-dihydro-2*H*-1,4-benzothiazin-3-one, (II), (Ellouz *et al.*, 2017*a*) and (*2Z*)-2-[(4-fluorobenzylidene)-4-(prop-2-yn-1-yl)-3,4-dihydro-2*H*-1,4-benzothiazin-3-one, (III), (Hni *et al.*, 2019), and they are nearly the same as those in (*2Z*)-4-[2-(2-oxo-1,3-oxazolidin-3-yl)ethyl]-2(phenylmethylidene)-3,4-dihydro-2*H*-1,4-benzothiazin-3-one, (IV), (Sebbar *et al.*, 2016*a*), where the heterocyclic portions of the dihydrobenzothiazine units are planar in (IV) and non-planar in (II) and (III).

3. Supramolecular features

In the crystal, the molecules form stacks extending along the normal to (104) through π -stacking interactions between *C*7=O1 and the *C* ring at $-x + 1, -y + 1, -z + 1$ [$\text{O}1 \cdots \text{centroid} = 3.2744(16)$ Å, $\text{C}7 \cdots \text{centroid} = 3.5448(18)$ Å and $\text{C}7=\text{O}1 \cdots \text{centroid} = 92.4(1)^\circ$] and between *C*13=O3 and the *C* ring at $-x + 1, -y + 1, -z$ [$\text{O}3 \cdots \text{centroid} = 3.3332(15)$ Å, $\text{C}13 \cdots \text{centroid} = 3.4800(18)$ Å and $\text{C}13=\text{O}3 \cdots \text{centroid} = 86.7(1)^\circ$] (Figs. 2 and 3). Intercalation of the aromatic rings between stacks (Fig. 4) leads to an

**Figure 3**

A partial packing diagram viewed along the b -axis direction with the π -stacking interactions shown by dashed lines.

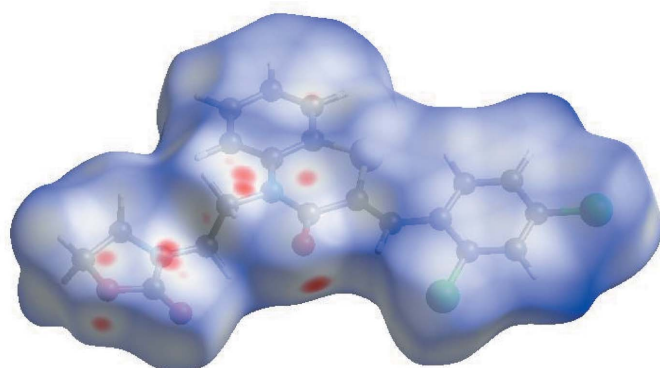
**Figure 4**

A partial packing diagram viewed along the c -axis direction with the π -stacking interactions shown by dashed lines.

overall layer structure with the layers approximately parallel to (101) (Fig. 3).

4. Hirshfeld surface analysis

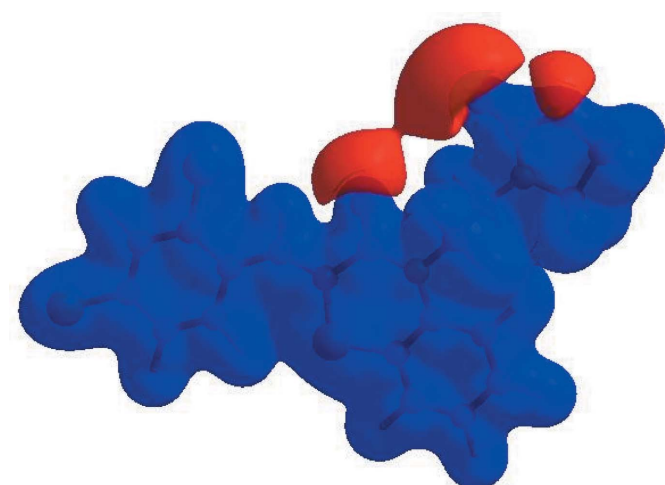
In order to visualize the intermolecular interactions in the crystal of the title compound, a Hirshfeld surface (HS) analysis (Hirshfeld, 1977; Spackman & Jayatilaka, 2009) was carried out by using *CrystalExplorer17.5* (Turner *et al.*, 2017). In the HS plotted over d_{norm} (Fig. 5), the white surface indicates contacts with distances equal to the sum of van der Waals radii, and the red and blue colours indicate distances shorter

**Figure 5**

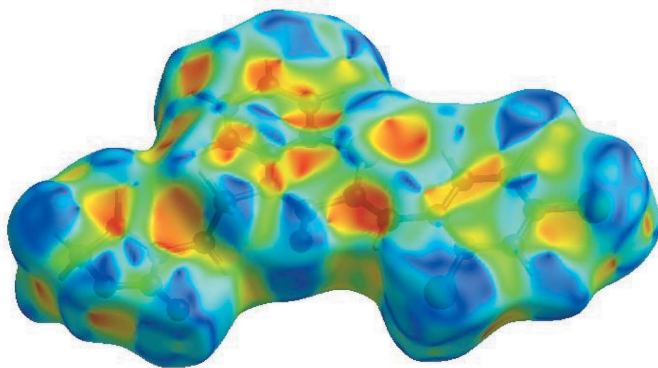
View of the three-dimensional Hirshfeld surface of the title compound plotted over d_{norm} in the range -0.1152 to 1.5656 a.u.

(in close contact) or longer (distinct contact) than the van der Waals radii, respectively (Venkatesan *et al.*, 2016). The bright-red spots indicate their roles as the respective donors and/or acceptors; they also appear as blue and red regions corresponding to positive and negative potentials on the HS mapped over electrostatic potential (Spackman *et al.*, 2008; Jayatilaka *et al.*, 2005), as shown in Fig. 6. The blue regions indicate positive electrostatic potential (hydrogen-bond donors), while the red regions indicate negative electrostatic potential (hydrogen-bond acceptors). The shape-index of the HS is a tool to visualize the π – π stacking by the presence of adjacent red and blue triangles; if there are no adjacent red and/or blue triangles, then there are no $\pi_{\text{ring}}\text{--}\pi_{\text{ring}}$ interactions. Fig. 7 clearly suggest that there are no π – π interactions in (I).

The overall two-dimensional fingerprint plot, Fig. 8*a*, and those delineated into $\text{H}\cdots\text{H}$, $\text{H}\cdots\text{Cl/Cl}\cdots\text{H}$, $\text{H}\cdots\text{O/O}\cdots\text{H}$, $\text{H}\cdots\text{C/C}\cdots\text{H}$, $\text{C}\cdots\text{C}$, $\text{H}\cdots\text{S/S}\cdots\text{H}$, $\text{C}\cdots\text{Cl/Cl}\cdots\text{C}$, $\text{S}\cdots\text{Cl/$

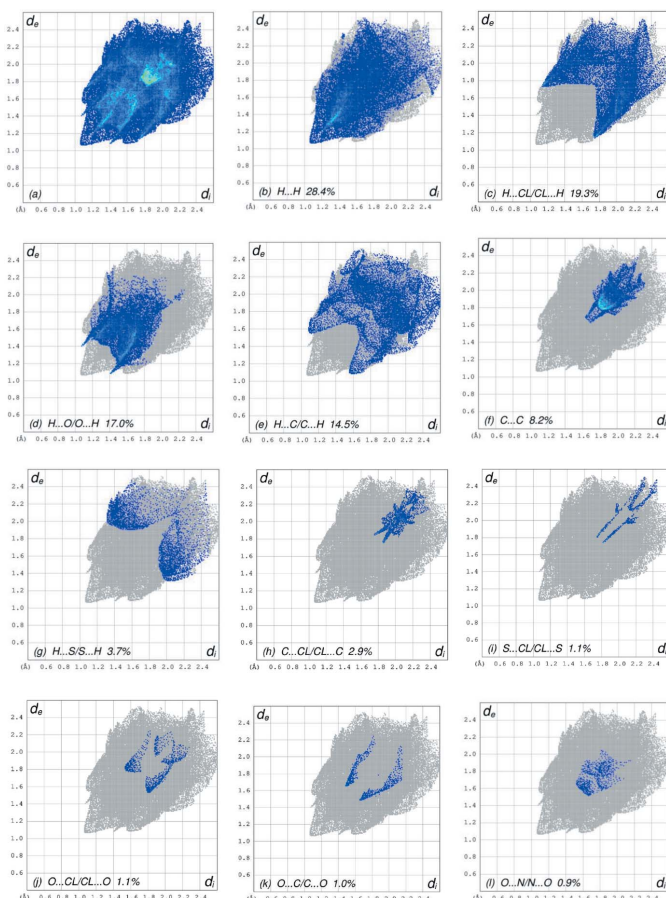
**Figure 6**

View of the three-dimensional Hirshfeld surface of the title compound plotted over electrostatic potential energy in the range -0.0500 to 0.0500 a.u. using the STO-3 G basis set at the Hartree–Fock level of theory. Hydrogen-bond donors and acceptors are shown as blue and red regions around the atoms, corresponding to positive and negative potentials, respectively.

**Figure 7**

Hirshfeld surface of the title compound plotted over shape-index.

$\text{Cl}\cdots\text{S}$, $\text{O}\cdots\text{Cl}/\text{Cl}\cdots\text{O}$, $\text{O}\cdots\text{C/C}\cdots\text{O}$ and $\text{O}\cdots\text{N/N}\cdots\text{O}$ contacts (McKinnon *et al.*, 2007) are illustrated in Fig. 8*b–l*, respectively, together with their relative contributions to the Hirshfeld surface. The most important interaction is $\text{H}\cdots\text{H}$

**Figure 8**

The full two-dimensional fingerprint plots for the title compound, showing (a) all interactions, and delineated into (b) $\text{H}\cdots\text{H}$, (c) $\text{H}\cdots\text{Cl}/\text{Cl}\cdots\text{H}$, (d) $\text{H}\cdots\text{O/O}\cdots\text{H}$, (e) $\text{H}\cdots\text{C/C}\cdots\text{H}$, (f) $\text{C}\cdots\text{C}$, (g) $\text{H}\cdots\text{S/S}\cdots\text{H}$, (h) $\text{C}\cdots\text{Cl/Cl}\cdots\text{C}$, (i) $\text{S}\cdots\text{Cl/Cl}\cdots\text{S}$, (j) $\text{O}\cdots\text{Cl/Cl}\cdots\text{O}$, (k) $\text{O}\cdots\text{C/C}\cdots\text{O}$ and (l) $\text{O}\cdots\text{N/N}\cdots\text{O}$ interactions. The d_i and d_e values are the closest internal and external distances (in Å) from given points on the Hirshfeld surface contacts.

Table 1
Selected interatomic distances (Å).

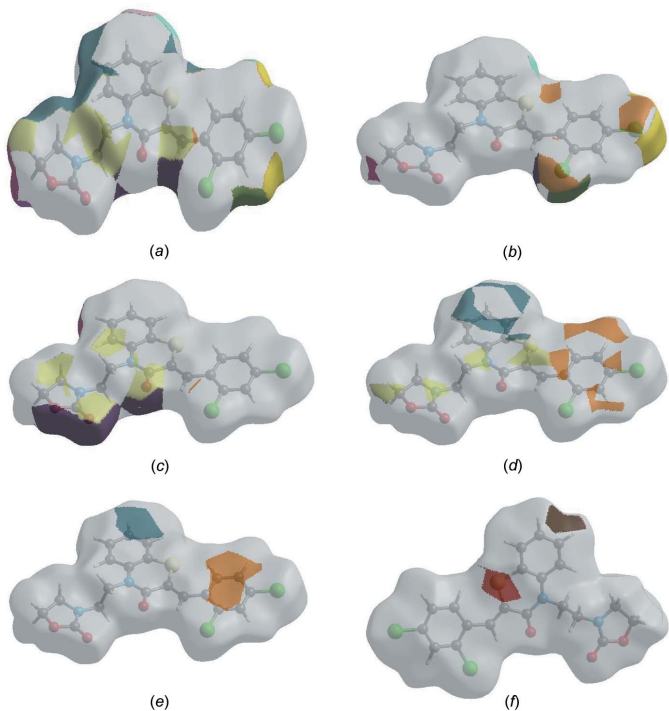
$\text{Cl}1\cdots\text{S}1^{\text{i}}$	3.5625 (7)	$\text{O}3\cdots\text{H}10B$	2.61 (2)
$\text{Cl}2\cdots\text{C}12^{\text{ii}}$	3.470 (2)	$\text{O}3\cdots\text{H}5^{\text{ii}}$	2.78 (2)
$\text{Cl}2\cdots\text{C}3^{\text{iii}}$	3.557 (2)	$\text{O}3\cdots\text{H}11B^{\text{ii}}$	2.80 (2)
$\text{Cl}2\cdots\text{O}2^{\text{ii}}$	3.3371 (13)	$\text{O}3\cdots\text{H}9A^{\text{v}}$	2.73 (2)
$\text{Cl}1\cdots\text{H}3^{\text{iv}}$	3.01 (3)	$\text{O}3\cdots\text{H}9B^{\text{v}}$	2.90 (2)
$\text{Cl}1\cdots\text{H}16^{\text{i}}$	2.97 (3)	$\text{O}3\cdots\text{H}11A^{\text{vi}}$	2.82 (2)
$\text{Cl}2\cdots\text{H}14$	2.51 (2)	$\text{N}2\cdots\text{O}3^{\text{vi}}$	3.165 (2)
$\text{Cl}2\cdots\text{H}4^{\text{iii}}$	3.12 (2)	$\text{N}2\cdots\text{C}13^{\text{vi}}$	3.190 (2)
$\text{Cl}2\cdots\text{H}12A^{\text{ii}}$	3.15 (2)	$\text{N}2\cdots\text{H}9B^{\text{v}}$	2.91 (2)
$\text{Cl}2\cdots\text{H}3^{\text{iii}}$	2.97 (3)	$\text{C}5\cdots\text{C}10$	3.422 (3)
$\text{S}1\cdots\text{N}1$	3.1231 (14)	$\text{C}7\cdots\text{C}12^{\text{v}}$	3.580 (3)
$\text{S}1\cdots\text{C}16$	3.136 (2)	$\text{C}9\cdots\text{C}13^{\text{v}}$	3.287 (2)
$\text{S}1\cdots\text{H}16$	2.45 (2)	$\text{C}10\cdots\text{C}13^{\text{vi}}$	3.369 (2)
$\text{O}1\cdots\text{C}10$	3.187 (2)	$\text{C}13\cdots\text{C}13^{\text{vi}}$	3.320 (2)
$\text{O}1\cdots\text{C}12^{\text{ii}}$	3.038 (2)	$\text{C}5\cdots\text{H}10A$	2.97 (2)
$\text{O}1\cdots\text{C}12^{\text{v}}$	3.304 (3)	$\text{C}5\cdots\text{H}9A$	2.53 (2)
$\text{O}2\cdots\text{C}10^{\text{vi}}$	3.255 (2)	$\text{C}7\cdots\text{H}10B$	2.99 (2)
$\text{O}2\cdots\text{C}7^{\text{v}}$	3.143 (2)	$\text{C}8\cdots\text{H}16$	2.99 (2)
$\text{O}3\cdots\text{N}2^{\text{vi}}$	3.165 (2)	$\text{C}9\cdots\text{H}5$	2.52 (2)
$\text{O}3\cdots\text{C}11^{\text{vi}}$	3.328 (3)	$\text{C}9\cdots\text{H}9B^{\text{v}}$	2.92 (2)
$\text{O}3\cdots\text{C}11^{\text{ii}}$	3.375 (2)	$\text{C}10\cdots\text{H}5$	2.92 (2)
$\text{O}3\cdots\text{C}9^{\text{v}}$	3.196 (2)	$\text{C}13\cdots\text{H}9B^{\text{v}}$	2.70 (2)
$\text{O}1\cdots\text{H}12B^{\text{ii}}$	2.75 (2)	$\text{C}14\cdots\text{H}12B^{\text{v}}$	2.98 (2)
$\text{O}1\cdots\text{H}9B$	2.23 (2)	$\text{H}5\cdots\text{H}9A$	2.06 (3)
$\text{O}1\cdots\text{H}10B$	2.73 (2)	$\text{H}5\cdots\text{H}10A$	2.49 (3)
$\text{O}1\cdots\text{H}12A^{\text{ii}}$	2.74 (2)	$\text{H}9A\cdots\text{H}11B$	2.58 (3)
$\text{O}1\cdots\text{H}12B^{\text{v}}$	2.79 (2)	$\text{H}9B\cdots\text{H}9B^{\text{v}}$	2.26 (3)
$\text{O}1\cdots\text{H}14$	2.23 (2)	$\text{H}10A\cdots\text{H}11A$	2.58 (3)
$\text{O}2\cdots\text{H}10B^{\text{vi}}$	2.75 (2)	$\text{H}10B\cdots\text{H}12A^{\text{vi}}$	2.45 (3)
$\text{O}2\cdots\text{H}4^{\text{ii}}$	2.62 (2)	$\text{H}12A\cdots\text{H}10B^{\text{vi}}$	2.45 (3)

Symmetry codes: (i) $-x, y + \frac{1}{2}, -z + \frac{3}{2}$; (ii) $-x + 1, y + \frac{1}{2}, -z + \frac{1}{2}$; (iii) $x, y + 1, z$; (iv) $-x, -y + 1, -z + 1$; (v) $-x + 1, -y + 1, -z + 1$; (vi) $-x + 1, -y + 1, -z$.

(Table 1) contributing 28.4% to the overall crystal packing, which is reflected in Fig. 8*b* as widely scattered points of high density with the tip at $d_e = d_i = 1.06$ Å. The pair of the scattered points of wings in the fingerprint plot delineated into $\text{H}\cdots\text{Cl/Cl}\cdots\text{H}$ contacts (19.3% contribution to the HS) have a nearly symmetrical distribution of points, Fig. 8*c*, with thin edges at $d_e + d_i = 2.88$ Å. The fingerprint plot delineated into $\text{H}\cdots\text{O/O}\cdots\text{H}$ contacts (17.0%), Fig. 8*d*, has a pair of characteristic wings with a pair of spikes with the tips at $d_e + d_i = 2.48$ Å. In the absence of $\text{C}\cdots\text{H}\cdots\pi$ interactions, the pair of wings in the fingerprint plot delineated into $\text{H}\cdots\text{C/C}\cdots\text{H}$ contacts (14.5%) have a nearly symmetrical distribution of points, Fig. 8*e*, with thick edges at $d_e + d_i \sim 2.66$ Å. The $\text{C}\cdots\text{C}$ contacts (8.2%), Fig. 8*f*, have an arrow-shaped distribution of points with the tip at $d_e = d_i \sim 1.68$ Å. Finally, the $\text{H}\cdots\text{S/S}\cdots\text{H}$ (Fig. 8*g*) and $\text{C}\cdots\text{Cl/Cl}\cdots\text{C}$ (Fig. 8*h*) contacts (3.7% and 2.9%, respectively), and are seen as pairs of wide and thin spikes with the tips at $d_e + d_i = 3.30$ and 3.60 Å, respectively.

The Hirshfeld surface representations with the function d_{norm} plotted onto the surface are shown for the $\text{H}\cdots\text{H}$, $\text{H}\cdots\text{Cl/Cl}\cdots\text{H}$, $\text{H}\cdots\text{O/O}\cdots\text{H}$, $\text{H}\cdots\text{C/C}\cdots\text{H}$, $\text{C}\cdots\text{C}$ and $\text{H}\cdots\text{S/S}\cdots\text{H}$ interactions in Fig. 9*a–f*, respectively.

The Hirshfeld surface analysis confirms the importance of H-atom contacts in establishing the packing. The large number of $\text{H}\cdots\text{H}$, $\text{H}\cdots\text{C/C}\cdots\text{H}$, $\text{H}\cdots\text{C/C}\cdots\text{H}$ and $\text{H}\cdots\text{O/O}\cdots\text{H}$ interactions suggest that van der Waals interactions and hydrogen bonding play the major roles in the crystal packing (Hathwar *et al.*, 2015).

**Figure 9**

The Hirshfeld surface representations with the function d_{norm} plotted onto the surface for (a) H···H, (b) H···Cl/Cl···H, (c) H···O/O···H, (d) H···C/C···H, (e) C···C and (f) H···S/S···H interactions.

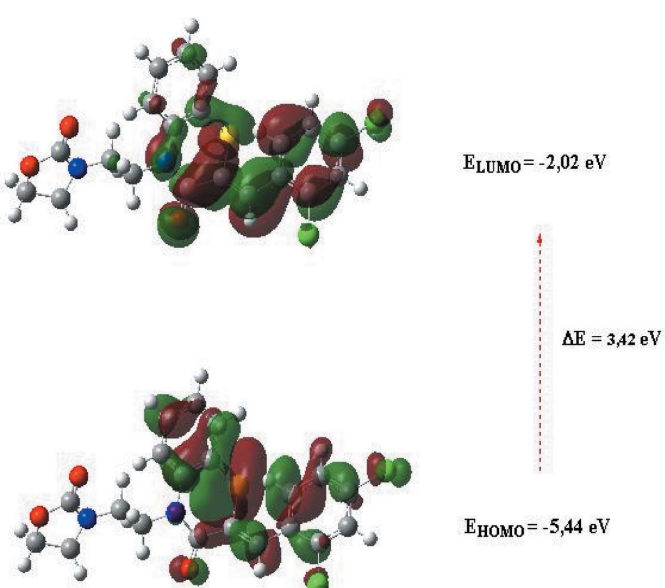
5. DFT calculations

The optimized structure of the title compound, (**I**), in the gas phase was generated theoretically *via* density functional theory (DFT) using standard B3LYP functional and 6-311 G(d,p) basis-set calculations (Becke, 1993) as implemented in *GAUSSIAN 09* (Frisch *et al.*, 2009). The theoretical and experimental results were in good agreement. The

highest-occupied molecular orbital (HOMO), acting as an electron donor, and the lowest-unoccupied molecular orbital (LUMO), acting as an electron acceptor, are very important parameters for quantum chemistry. When the energy gap is small, the molecule is highly polarizable and has high chemical reactivity. The electron transition from the HOMO to the LUMO energy level is shown in Fig. 10. The HOMO and LUMO are localized in the plane extending from the whole (2Z)-2-[(2,4-dichlorophenyl)methylidene]-4-[2-(2-oxo-1,3-oxazolidin-3-yl)ethyl]3,4-dihydro-2H-1,4-benzothiazin-3-one ring. The energy band gap [$\Delta E = E_{\text{LUMO}} - E_{\text{HOMO}}$] of the molecule is about 3.42 eV, and the frontier molecular orbital energies, E_{HOMO} and E_{LUMO} are -5.44 and -2.02 eV, respectively.

6. Database survey

A search of the Cambridge Crystallographic Database (Groom *et al.*, 2016; updated to Nov. 2018) using the fragment **II** ($R_1 = \text{Ph}$, $R_2 = \text{C}$; Fig. 11) gave 14 hits with $R_1 = \text{Ph}$ and $R_2 = \text{CH}_2\text{COOH}$ (Sebbar *et al.*, 2016c), *n*-octadecyl (Sebbar *et al.*, 2017a), $\text{CH}_2\text{C}\equiv\text{CH}$ (Sebbar *et al.*, 2014a), **IIa** (Sebbar *et al.*, 2016a), CH_2COOEt (Zerzouf *et al.*, 2001), **IIb** (Ellouz *et al.*, 2015a), *n*-Bu (Sebbar *et al.*, 2014b), **IIc** (Sebbar *et al.*, 2016d), Me (Ellouz *et al.*, 2015b) and **IID** (Sebbar *et al.*, 2015). In addition, there are structures with $R_1 = 4\text{-ClC}_6\text{H}_4$ and $R_2 = \text{CH}_2\text{Ph}_2$ (Ellouz *et al.*, 2016c), *n*-Bu (Ellouz *et al.*, 2017a), **IIa** (Ellouz *et al.*, 2017c) and $R_1 = 2\text{-ClC}_6\text{H}_4$, $R_2 = \text{CH}_2\text{C}\equiv\text{CH}$ (Sebbar *et al.*, 2017b). In the majority of these, the heterocyclic ring is quite non-planar with the dihedral angle between the plane defined by the benzene ring plus the nitrogen and sulfur atoms and that defined by nitrogen and sulfur and the other two carbon atoms separating them ranging from *ca* 29° in $\text{CH}_2\text{C}\equiv\text{CH}$ (Sebbar *et al.*, 2014a), to 36° in **IID** (Sebbar *et al.*, 2015), which includes the value of *ca* 30° for 2*H*-1,4-benzothiazin-3(4*H*)-one (WAKLUQ 01; Merola, 2013). The other three (**IIa**, **IIc** and $R_1 = 4\text{-ClC}_6\text{H}_4$ and $R_2 = \text{CH}_2\text{Ph}_2$; Ellouz *et al.*, 2016c) have the benzothiazine unit nearly planar with a corresponding dihedral angle of *ca* $3\text{--}4^\circ$. In the case of **IIa**, the displacement ellipsoid for the sulfur atom shows a considerable elongation perpendicular to the mean plane of the heterocyclic ring, suggesting disorder, and a greater degree of non-planarity, but for the other two, there is no obvious source for the near planarity.

**Figure 10**

The energy-band gap of the title compound.

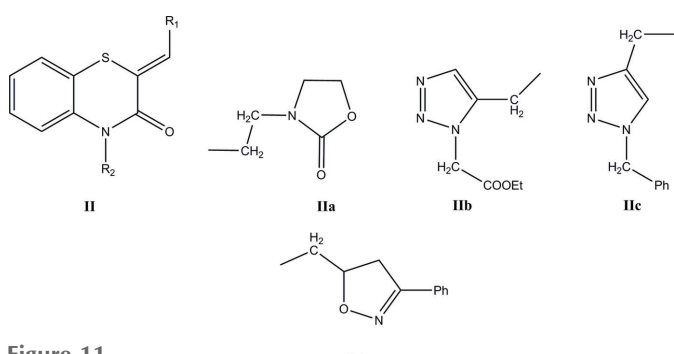
**Figure 11**
Related structures.

Table 2
Experimental details.

Crystal data	
Chemical formula	C ₂₀ H ₁₆ Cl ₂ N ₂ O ₃ S
M _r	435.31
Crystal system, space group	Monoclinic, P2 ₁ /c
Temperature (K)	150
a, b, c (Å)	18.4615 (8), 12.8567 (5), 7.9251 (4)
β (°)	96.926 (2)
V (Å ³)	1867.33 (14)
Z	4
Radiation type	Cu Kα
μ (mm ⁻¹)	4.40
Crystal size (mm)	0.21 × 0.12 × 0.05
Data collection	
Diffractometer	Bruker D8 VENTURE PHOTON 100 CMOS
Absorption correction	Numerical (<i>SADABS</i> ; Krause <i>et al.</i> , 2015)
T _{min} , T _{max}	0.51, 0.80
No. of measured, independent and observed [I > 2σ(I)] reflections	14033, 3678, 3252
R _{int}	0.032
(sin θ/λ) _{max} (Å ⁻¹)	0.619
Refinement	
R[F ² > 2σ(F ²)], wR(F ²), S	0.035, 0.093, 1.05
No. of reflections	3678
No. of parameters	317
H-atom treatment	All H-atom parameters refined
Δρ _{max} , Δρ _{min} (e Å ⁻³)	0.37, -0.38

Computer programs: *APEX3* and *SAINT* (Bruker, 2016), *SHELXT* (Sheldrick, 2015a), *SHELXL2018/1* (Sheldrick, 2015b), *DIAMOND* (Brandenburg & Putz, 2012) and *SHELXTL* (Sheldrick, 2008).

7. Synthesis and crystallization

Tetra-*n*-butylammonium bromide (0.1 mmol), 2.20 equiv. of bis(2-chloroethyl)amine hydrochloride and 2.00 equiv. of potassium carbonate were added to a solution of (*Z*)-2-(2,4-dichlorobenzylidene)-2*H*-1,4-benzothiazin-3(4*H*)-one (1.5 mmol) in DMF (25 ml). The mixture was stirred at 353 K for 6 h. After removal of salts by filtration, the solution was evaporated under reduced pressure and the residue obtained was dissolved in dichloromethane. The remaining salts were extracted with distilled water. The residue obtained was chromatographed on a silica gel column (eluent: ethyl acetate/hexane: 3/2). The isolated solid was recrystallized from ethanol solution to afford colourless crystals [light yellow in CIF?] (yield: 67%).

8. Refinement

Crystal data, data collection and structure refinement details are summarized in Table 2. Hydrogen atoms were located in a difference-Fourier map, and freely refined.

Funding information

The support of NSF-MRI grant No. 1228232 for the purchase of the diffractometer and Tulane University for support of the Tulane Crystallography Laboratory are gratefully acknowledged. TH is grateful to the Hacettepe University Scientific Research Project Unit (grant No. 013 D04 602 004).

References

- Aotsuka, T., Hosono, H., Kurihara, T., Nakamura, Y., Matsui, T. & Kobayashi, F. (1994). *Chem. Pharm. Bull.* **42**, 1264–1271.
 Armenise, D., Muraglia, M., Florio, M. A., Laurentis, N. D., Rosato, A., Carrieri, A., Corbo, F. & Franchini, C. (2012). *Mol. Pharmacol.* **50**, 1178–1188.
 Becke, A. D. (1993). *J. Chem. Phys.* **98**, 5648–5652.
 Brandenburg, K. & Putz, H. (2012). *DIAMOND*, Crystal Impact GbR, Bonn, Germany.
 Bruker (2016). *APEX3*, *SAINT* and *SADABS*. Bruker AXS, Inc., Madison, Wisconsin, USA.
 Ellouz, M., Elmselleem, H., Sebbar, N. K., Steli, H., Al Mamari, K., Nadeem, A., Ouzidan, Y., Essassi, E. M., Abdel-Rahaman, I. & Hristov, P. (2016b). *J. Mater. Environ. Sci.* **7**, 2482–2497.
 Ellouz, M., Sebbar, N. K., Boulhaoua, M., Essassi, E. M. & Mague, J. T. (2017a). *IUCr Data* **2**, x170646.
 Ellouz, M., Sebbar, N. K., Elmselleem, H., Steli, H., Fichtali, I., Mohamed, A. M. M., Mamari, K. A., Essassi, E. M. & Abdel-Rahaman, I. (2016a). *J. Mater. Environ. Sci.* **7**, 2806–2819.
 Ellouz, M., Sebbar, N. K., Essassi, E. M., Ouzidan, Y. & Mague, J. T. (2015a). *Acta Cryst. E71*, o1022–o1023.
 Ellouz, M., Sebbar, N. K., Essassi, E. M., Ouzidan, Y., Mague, J. T. & Zouhri, H. (2016c). *IUCrData*, **1**, x160764.
 Ellouz, M., Sebbar, N. K., Essassi, E. M., Saadi, M. & El Ammari, L. (2015b). *Acta Cryst. E71*, o862–o863.
 Ellouz, M., Sebbar, N. K., Ouzidan, Y., Essassi, E. M. & Mague, J. T. (2017b). *IUCrData*, **2**, x170097.
 Ellouz, M., Sebbar, N. K., Ouzidan, Y., Kaur, M., Essassi, E. M. & Jasinski, J. P. (2017c). *IUCrData*, **2**, x170870.
 Frisch, M. J., Trucks, G. W., Schlegel, H. B., Scuseria, G. E., Robb, M. A., Cheeseman, J. R., *et al.* (2009). *GAUSSIAN09*. Gaussian Inc., Wallingford, CT, USA.
 Fujimura, K., Ota, A. & Kawashima, Y. (1996). *Chem. Pharm. Bull.* **44**, 542–546.
 Groom, C. R., Bruno, I. J., Lightfoot, M. P. & Ward, S. C. (2016). *Acta Cryst. B72*, 171–179.
 Gupta, R. R. & Kumar, R. (1986). *J. Fluor. Chem.* **31**, 19–24.
 Hathwar, V. R., Sist, M., Jørgensen, M. R. V., Mamakhe, A. H., Wang, X., Hoffmann, C. M., Sugimoto, K., Overgaard, J. & Iversen, B. B. (2015). *IUCrJ*, **2**, 563–574.
 Hirshfeld, H. L. (1977). *Theor. Chim. Acta*, **44**, 129–138.
 Hni, B., Sebbar, N. K., Hökelek, T., Ouzidan, Y., Moussaif, A., Mague, J. T. & Essassi, E. M. (2019). *Acta Cryst. E75*, 372–377.
 Jayatilaka, D., Grimwood, D. J., Lee, A., Lemay, A., Russel, A. J., Taylor, C., Wolff, S. K., Cassam-Chenai, P. & Whitton, A. (2005). *TONTO - A System for Computational Chemistry*. Available at: <http://hirshfeldsurface.net/>
 Krause, L., Herbst-Irmer, R., Sheldrick, G. M. & Stalke, D. (2015). *J. Appl. Cryst.* **48**, 3–10.
 Malagu, K., Boustie, J., David, M., Sauleau, J., Amoros, M., Girre, R. L. & Sauleau, A. (1998). *Pharm. Pharmacol. Commun.* **4**, 57–60.
 McKinnon, J. J., Jayatilaka, D. & Spackman, M. A. (2007). *Chem. Commun.* pp. 3814.
 Merola, J. S. (2013). Private Communication (refcode 977080). CCDC, Cambridge, England.
 Rathore, B. S. & Kumar, M. (2006). *Bioorg. Med. Chem.* **14**, 5678–5682.
 Sabatini, S., Kaatz, G. W., Rossolini, G. M., Brandini, D. & Fravolini, A. (2008). *J. Med. Chem.* **51**, 4321–4330.
 Sebbar, N. K., El Fal, M., Essassi, E. M., Saadi, M. & El Ammari, L. (2014b). *Acta Cryst. E70*, o686.
 Sebbar, N. K., Ellouz, M., Boulhaoua, M., Ouzidan, Y., Essassi, E. M. & Mague, J. T. (2016d). *IUCrData*, **1**, x161823.
 Sebbar, N. K., Ellouz, M., Essassi, E. M., Saadi, M. & El Ammari, L. (2015). *Acta Cryst. E71*, o423–o424.
 Sebbar, N. K., Ellouz, M., Essassi, E. M., Saadi, M. & El Ammari, L. (2016b). *IUCrData*, **1**, x161012.

- Sebbar, N. K., Ellouz, M., Lahmudi, S., Hlimi, F., Essassi, E. & Mague, J. T. (2017a). *IUCrData*, **2**, x170695.
- Sebbar, N. K., Ellouz, M., Mague, J. T., Ouzidan, Y., Essassi, E. M. & Zouihri, H. (2016c). *IUCrData*, **1**, x160863.
- Sebbar, N. K., Ellouz, M., Ouzidan, Y., Kaur, M., Essassi, E. M. & Jasinski, J. P. (2017b). *IUCr Data* **2**, x170889.
- Sebbar, N. K., Mekhzoum, M. E. M., Essassi, E. M., Zerzouf, A., Talbaoui, A., Bakri, Y., Saadi, M. & Ammari, L. E. (2016a). *Res. Chem. Intermed.* **42**, 6845–6862.
- Sebbar, N. K., Zerzouf, A., Essassi, E. M., Saadi, M. & El Ammari, L. (2014a). *Acta Cryst. E* **70**, o614.
- Sheldrick, G. M. (2008). *Acta Cryst. A* **64**, 112–122.
- Sheldrick, G. M. (2015a). *Acta Cryst. A* **71**, 3–8.
- Sheldrick, G. M. (2015b). *Acta Cryst. C* **71**, 3–8.
- Spackman, M. A. & Jayatilaka, D. (2009). *CrystEngComm*, **11**, 19–32.
- Spackman, M. A., McKinnon, J. J. & Jayatilaka, D. (2008). *Cryst. Eng. Comm*, **10**, 377–388.
- Takemoto, I., Yamasaki, K. & Kaminaka, H. (1994). *Biosci. Biotechnol. Biochem.* **58**, 788–789.
- Tawada, H., Sugiyama, Y., Ikeda, H., Yamamoto, Y. & Meguro, K. (1990). *Chem. Pharm. Bull.* **38**, 1238–1245.
- Turner, M. J., McKinnon, J. J., Wolff, S. K., Grimwood, D. J., Spackman, P. R., Jayatilaka, D. & Spackman, M. A. (2017). *CrystExplor17*. The University of Western Australia.
- Venkatesan, P., Thamotharan, S., Ilangoan, A., Liang, H. & Sundius, T. (2016). *Spectrochim. Acta Part A*, **153**, 625–636.
- Vidal, A., Madelmont, J. C. & Mounetou, E. A. (2006). *Synthesis*, pp. 591–593.
- Wammack, R., Remzi, M., Seitz, C., Djavan, B. & Marberger, M. (2002). *Eur. Urol.* **41**, 596–601.
- Warren, B. K. & Knaus, E. E. (1987). *Eur. J. Med. Chem.* **22**, 411–415.
- Zerzouf, A., Salem, M., Essassi, E. M. & Pierrot, M. (2001). *Acta Cryst. E* **57**, o498–o499.
- Zia-ur-Rehman, M., Choudary, J. A., Elsegood, M. R. J., Siddiqui, H. L. & Khan, K. M. (2009). *Eur. J. Med. Chem.* **44**, 1311–1316.

supporting information

Acta Cryst. (2019). E75, 593-599 [https://doi.org/10.1107/S2056989019004250]

Crystal structure, Hirshfeld surface analysis and DFT study of (2Z)-2-(2,4-di-chlorobenzylidene)-4-[2-(2-oxo-1,3-oxazolidin-3-yl)ethyl]-3,4-dihydro-2H-1,4-benzothiazin-3-one

Brahim Hni, Nada Kheira Sebbar, Tuncer Hökelek, Lhoussaine El Ghayati, Younes Bouzian, Joel T. Mague and El Mokhtar Essassi

Computing details

Data collection: *APEX3* (Bruker, 2016); cell refinement: *SAINT* (Bruker, 2016); data reduction: *SAINT* (Bruker, 2016); program(s) used to solve structure: *SHELXT* (Sheldrick, 2015a); program(s) used to refine structure: *SHELXL2018/1* (Sheldrick, 2015b); molecular graphics: *DIAMOND* (Brandenburg & Putz, 2012); software used to prepare material for publication: *SHELXTL* (Sheldrick, 2008).

(2Z)-2-(2,4-Dichlorobenzylidene)-4-[2-(2-oxo-1,3-oxazolidin-3-yl)ethyl]-3,4-dihydro-2H-1,4-benzothiazin-3-one

Crystal data

$C_{20}H_{16}Cl_2N_2O_3S$
 $M_r = 435.31$
Monoclinic, $P2_1/c$
 $a = 18.4615 (8)$ Å
 $b = 12.8567 (5)$ Å
 $c = 7.9251 (4)$ Å
 $\beta = 96.926 (2)^\circ$
 $V = 1867.33 (14)$ Å³
 $Z = 4$

$F(000) = 896$
 $D_x = 1.548 \text{ Mg m}^{-3}$
Cu $K\alpha$ radiation, $\lambda = 1.54178$ Å
Cell parameters from 9952 reflections
 $\theta = 3.5\text{--}72.5^\circ$
 $\mu = 4.39 \text{ mm}^{-1}$
 $T = 150$ K
Column, light yellow
0.21 × 0.12 × 0.05 mm

Data collection

Bruker D8 VENTURE PHOTON 100 CMOS
diffractometer
Radiation source: INCOATEC I μ S micro-focus
source
Mirror monochromator
Detector resolution: 10.4167 pixels mm⁻¹
 ω scans
Absorption correction: numerical
(SADABS; Krause *et al.*, 2015)

$T_{\min} = 0.51$, $T_{\max} = 0.80$
14033 measured reflections
3678 independent reflections
3252 reflections with $I > 2\sigma(I)$
 $R_{\text{int}} = 0.032$
 $\theta_{\max} = 72.5^\circ$, $\theta_{\min} = 2.4^\circ$
 $h = -22 \rightarrow 21$
 $k = -14 \rightarrow 15$
 $l = -9 \rightarrow 9$

Refinement

Refinement on F^2
Least-squares matrix: full
 $R[F^2 > 2\sigma(F^2)] = 0.035$
 $wR(F^2) = 0.093$
 $S = 1.05$

3678 reflections
317 parameters
0 restraints
Primary atom site location: structure-invariant
direct methods

Secondary atom site location: difference Fourier map

$$w = 1/[\sigma^2(F_o^2) + (0.0467P)^2 + 0.9972P]$$

$$\text{where } P = (F_o^2 + 2F_c^2)/3$$

Hydrogen site location: difference Fourier map

$$(\Delta/\sigma)_{\max} = 0.001$$

All H-atom parameters refined

$$\Delta\rho_{\max} = 0.37 \text{ e \AA}^{-3}$$

$$\Delta\rho_{\min} = -0.38 \text{ e \AA}^{-3}$$

Special details

Geometry. All esds (except the esd in the dihedral angle between two l.s. planes) are estimated using the full covariance matrix. The cell esds are taken into account individually in the estimation of esds in distances, angles and torsion angles; correlations between esds in cell parameters are only used when they are defined by crystal symmetry. An approximate (isotropic) treatment of cell esds is used for estimating esds involving l.s. planes.

Refinement. Refinement of F^2 against ALL reflections. The weighted R-factor wR and goodness of fit S are based on F^2 , conventional R-factors R are based on F, with F set to zero for negative F^2 . The threshold expression of $F^2 > 2\text{sigma}(F^2)$ is used only for calculating R-factors(gt) etc. and is not relevant to the choice of reflections for refinement. R-factors based on F^2 are statistically about twice as large as those based on F, and R-factors based on ALL data will be even larger.

Fractional atomic coordinates and isotropic or equivalent isotropic displacement parameters (\AA^2)

	x	y	z	$U_{\text{iso}}^*/U_{\text{eq}}$
C11	-0.02396 (3)	0.92135 (4)	0.75404 (8)	0.05021 (17)
Cl2	0.23463 (3)	0.91630 (3)	0.51698 (8)	0.04067 (15)
S1	0.17782 (2)	0.48226 (3)	0.53284 (7)	0.03232 (14)
O1	0.35726 (7)	0.62658 (10)	0.44041 (18)	0.0330 (3)
O2	0.61496 (6)	0.46053 (10)	0.16700 (16)	0.0267 (3)
O3	0.54282 (7)	0.59880 (10)	0.19909 (16)	0.0299 (3)
N1	0.33467 (7)	0.45458 (11)	0.42952 (18)	0.0227 (3)
N2	0.49920 (8)	0.43048 (11)	0.19710 (19)	0.0240 (3)
C1	0.21852 (9)	0.36941 (13)	0.4668 (2)	0.0237 (3)
C2	0.17612 (10)	0.27967 (14)	0.4671 (3)	0.0298 (4)
H2	0.1287 (13)	0.2873 (18)	0.496 (3)	0.036 (6)*
C3	0.20375 (10)	0.18467 (15)	0.4260 (3)	0.0328 (4)
H3	0.1739 (14)	0.125 (2)	0.424 (3)	0.043 (6)*
C4	0.27384 (10)	0.17928 (14)	0.3800 (2)	0.0299 (4)
H4	0.2935 (12)	0.1146 (19)	0.352 (3)	0.037 (6)*
C5	0.31603 (10)	0.26806 (14)	0.3770 (2)	0.0255 (4)
H5	0.3619 (13)	0.2616 (18)	0.342 (3)	0.035 (6)*
C6	0.28970 (9)	0.36498 (13)	0.4241 (2)	0.0221 (3)
C7	0.31385 (9)	0.55557 (13)	0.4532 (2)	0.0238 (3)
C8	0.23937 (9)	0.57999 (13)	0.5014 (2)	0.0233 (3)
C9	0.41197 (9)	0.44207 (14)	0.4043 (2)	0.0235 (3)
H9A	0.4306 (11)	0.3741 (17)	0.457 (3)	0.029 (5)*
H9B	0.4388 (11)	0.4975 (17)	0.468 (3)	0.028 (5)*
C10	0.42367 (9)	0.45187 (15)	0.2187 (2)	0.0264 (4)
H10A	0.3897 (12)	0.4031 (17)	0.146 (3)	0.031 (5)*
H10B	0.4108 (12)	0.5235 (18)	0.181 (3)	0.033 (6)*
C11	0.52850 (10)	0.32643 (14)	0.1876 (3)	0.0285 (4)
H11A	0.4991 (13)	0.2859 (18)	0.099 (3)	0.038 (6)*
H11B	0.5292 (13)	0.2906 (19)	0.295 (3)	0.043 (6)*
C12	0.60490 (10)	0.34916 (14)	0.1433 (2)	0.0272 (4)

H12A	0.6082 (12)	0.3331 (18)	0.024 (3)	0.037 (6)*
H12B	0.6420 (13)	0.3167 (19)	0.219 (3)	0.039 (6)*
C13	0.54980 (9)	0.50543 (13)	0.1887 (2)	0.0227 (3)
C14	0.22602 (9)	0.68205 (14)	0.5250 (2)	0.0246 (4)
H14	0.2654 (11)	0.7266 (17)	0.504 (3)	0.027 (5)*
C15	0.16331 (9)	0.73590 (13)	0.5785 (2)	0.0241 (4)
C16	0.10234 (10)	0.68752 (15)	0.6352 (3)	0.0311 (4)
H16	0.0973 (13)	0.612 (2)	0.640 (3)	0.044 (7)*
C17	0.04455 (10)	0.74288 (16)	0.6871 (3)	0.0344 (4)
H17	0.0037 (15)	0.710 (2)	0.725 (3)	0.050 (7)*
C18	0.04662 (10)	0.84994 (16)	0.6841 (3)	0.0330 (4)
C19	0.10510 (10)	0.90291 (15)	0.6301 (3)	0.0325 (4)
H19	0.1073 (11)	0.9771 (19)	0.626 (3)	0.032 (6)*
C20	0.16222 (10)	0.84560 (14)	0.5794 (2)	0.0271 (4)

Atomic displacement parameters (\AA^2)

	U^{11}	U^{22}	U^{33}	U^{12}	U^{13}	U^{23}
Cl1	0.0335 (3)	0.0432 (3)	0.0774 (4)	0.0150 (2)	0.0207 (3)	-0.0079 (3)
Cl2	0.0354 (3)	0.0187 (2)	0.0718 (4)	-0.00040 (17)	0.0224 (2)	0.0036 (2)
S1	0.0250 (2)	0.0169 (2)	0.0593 (3)	-0.00047 (16)	0.0225 (2)	-0.00057 (19)
O1	0.0279 (6)	0.0224 (7)	0.0522 (8)	-0.0045 (5)	0.0198 (6)	-0.0021 (6)
O2	0.0227 (6)	0.0208 (6)	0.0390 (7)	-0.0020 (5)	0.0131 (5)	-0.0006 (5)
O3	0.0380 (7)	0.0183 (6)	0.0349 (7)	0.0008 (5)	0.0106 (5)	0.0001 (5)
N1	0.0187 (7)	0.0201 (7)	0.0308 (7)	0.0006 (5)	0.0097 (5)	-0.0007 (6)
N2	0.0224 (7)	0.0182 (7)	0.0338 (8)	-0.0002 (5)	0.0131 (6)	-0.0008 (6)
C1	0.0231 (8)	0.0175 (8)	0.0316 (9)	0.0011 (6)	0.0080 (7)	0.0013 (6)
C2	0.0232 (8)	0.0219 (9)	0.0454 (11)	-0.0026 (7)	0.0097 (7)	0.0003 (8)
C3	0.0306 (9)	0.0192 (9)	0.0493 (12)	-0.0039 (7)	0.0079 (8)	-0.0017 (8)
C4	0.0323 (9)	0.0187 (9)	0.0395 (10)	0.0027 (7)	0.0070 (8)	-0.0039 (7)
C5	0.0252 (8)	0.0221 (9)	0.0304 (9)	0.0036 (7)	0.0083 (7)	-0.0007 (7)
C6	0.0220 (8)	0.0183 (8)	0.0268 (8)	-0.0015 (6)	0.0060 (6)	0.0008 (6)
C7	0.0225 (8)	0.0186 (8)	0.0320 (9)	-0.0007 (6)	0.0105 (7)	0.0000 (7)
C8	0.0212 (8)	0.0187 (8)	0.0319 (9)	-0.0005 (6)	0.0103 (6)	0.0012 (6)
C9	0.0167 (7)	0.0272 (9)	0.0274 (8)	0.0014 (7)	0.0063 (6)	-0.0011 (7)
C10	0.0219 (8)	0.0298 (10)	0.0287 (9)	0.0022 (7)	0.0079 (7)	0.0010 (7)
C11	0.0294 (9)	0.0171 (8)	0.0412 (10)	-0.0003 (7)	0.0137 (8)	0.0007 (7)
C12	0.0280 (9)	0.0189 (8)	0.0365 (10)	0.0015 (7)	0.0116 (8)	-0.0030 (7)
C13	0.0257 (8)	0.0212 (8)	0.0224 (8)	-0.0008 (7)	0.0085 (6)	0.0008 (6)
C14	0.0217 (8)	0.0193 (8)	0.0346 (9)	-0.0008 (7)	0.0109 (7)	0.0007 (7)
C15	0.0229 (8)	0.0206 (8)	0.0299 (9)	0.0021 (6)	0.0075 (7)	0.0005 (7)
C16	0.0265 (9)	0.0236 (9)	0.0456 (11)	-0.0001 (7)	0.0143 (8)	-0.0021 (8)
C17	0.0255 (9)	0.0330 (10)	0.0475 (12)	0.0011 (8)	0.0155 (8)	-0.0029 (8)
C18	0.0255 (9)	0.0328 (10)	0.0416 (10)	0.0085 (8)	0.0087 (8)	-0.0040 (8)
C19	0.0311 (10)	0.0226 (9)	0.0445 (11)	0.0062 (7)	0.0070 (8)	-0.0002 (8)
C20	0.0250 (8)	0.0219 (9)	0.0353 (9)	0.0019 (7)	0.0070 (7)	0.0010 (7)

Geometric parameters (\AA , $\text{\textcircled{}}^{\circ}$)

C11—C18	1.7385 (19)	C7—C8	1.504 (2)
Cl2—C20	1.7373 (18)	C8—C14	1.352 (2)
S1—C8	1.7321 (17)	C9—C10	1.518 (2)
S1—C1	1.7430 (17)	C9—H9A	1.01 (2)
O1—C7	1.227 (2)	C9—H9B	0.97 (2)
O2—C13	1.364 (2)	C10—H10A	1.01 (2)
O2—C12	1.453 (2)	C10—H10B	0.99 (2)
O3—C13	1.211 (2)	C11—C12	1.522 (2)
N1—C7	1.374 (2)	C11—H11A	0.98 (2)
N1—C6	1.418 (2)	C11—H11B	0.97 (3)
N1—C9	1.473 (2)	C12—H12A	0.97 (2)
N2—C13	1.349 (2)	C12—H12B	0.95 (2)
N2—C11	1.448 (2)	C14—C15	1.455 (2)
N2—C10	1.451 (2)	C14—H14	0.96 (2)
C1—C2	1.394 (2)	C15—C16	1.406 (2)
C1—C6	1.397 (2)	C15—C20	1.411 (2)
C2—C3	1.378 (3)	C16—C17	1.386 (3)
C2—H2	0.94 (2)	C16—H16	0.97 (3)
C3—C4	1.388 (3)	C17—C18	1.377 (3)
C3—H3	0.94 (3)	C17—H17	0.95 (3)
C4—C5	1.384 (3)	C18—C19	1.387 (3)
C4—H4	0.94 (2)	C19—C20	1.385 (3)
C5—C6	1.404 (2)	C19—H19	0.96 (2)
C5—H5	0.93 (2)		
Cl1…S1 ⁱ	3.5625 (7)	O3…H10B	2.61 (2)
Cl2…C12 ⁱⁱ	3.470 (2)	O3…H5 ⁱⁱ	2.78 (2)
Cl2…C3 ⁱⁱⁱ	3.557 (2)	O3…H11B ⁱⁱ	2.80 (2)
Cl2…O2 ⁱⁱ	3.3371 (13)	O3…H9A ^v	2.73 (2)
Cl1…H3 ^{iv}	3.01 (3)	O3…H9B ^v	2.90 (2)
Cl1…H16 ⁱ	2.97 (3)	O3…H11A ^{vi}	2.82 (2)
Cl2…H14	2.51 (2)	N2…O3 ^{vi}	3.165 (2)
Cl2…H4 ⁱⁱⁱ	3.12 (2)	N2…C13 ^{vi}	3.190 (2)
Cl2…H12A ⁱⁱ	3.15 (2)	N2…H9B ^v	2.91 (2)
Cl2…H3 ⁱⁱⁱ	2.97 (3)	C5…C10	3.422 (3)
S1…N1	3.1231 (14)	C7…C12 ^v	3.580 (3)
S1…C16	3.136 (2)	C9…C13 ^v	3.287 (2)
S1…H16	2.45 (2)	C10…C13 ^{vi}	3.369 (2)
O1…C10	3.187 (2)	C13…C13 ^{vi}	3.320 (2)
O1…C12 ⁱⁱ	3.038 (2)	C5…H10A	2.97 (2)
O1…C12 ^v	3.304 (3)	C5…H9A	2.53 (2)
O2…C10 ^{vi}	3.255 (2)	C7…H10B	2.99 (2)
O2…C7 ^v	3.143 (2)	C8…H16	2.99 (2)
O3…N2 ^{vi}	3.165 (2)	C9…H5	2.52 (2)
O3…C11 ^{vi}	3.328 (3)	C9…H9B ^v	2.92 (2)
O3…C11 ⁱⁱ	3.375 (2)	C10…H5	2.92 (2)

O3···C9 ^v	3.196 (2)	C13···H9B ^v	2.70 (2)
O1···H12B ⁱⁱ	2.75 (2)	C14···H12B ^v	2.98 (2)
O1···H9B	2.23 (2)	H5···H9A	2.06 (3)
O1···H10B	2.73 (2)	H5···H10A	2.49 (3)
O1···H12A ⁱⁱ	2.74 (2)	H9A···H11B	2.58 (3)
O1···H12B ^v	2.79 (2)	H9B···H9B ^v	2.26 (3)
O1···H14	2.23 (2)	H10A···H11A	2.58 (3)
O2···H10B ^{vi}	2.75 (2)	H10B···H12A ^{vi}	2.45 (3)
O2···H4 ⁱⁱ	2.62 (2)	H12A···H10B ^{vi}	2.45 (3)
C8—S1—C1	104.29 (8)	C9—C10—H10A	110.3 (12)
C13—O2—C12	109.43 (13)	N2—C10—H10B	109.8 (13)
C7—N1—C6	126.86 (14)	C9—C10—H10B	108.4 (13)
C7—N1—C9	114.42 (14)	H10A—C10—H10B	107.1 (17)
C6—N1—C9	118.72 (14)	N2—C11—C12	101.36 (14)
C13—N2—C11	113.07 (14)	N2—C11—H11A	110.5 (13)
C13—N2—C10	123.45 (15)	C12—C11—H11A	112.7 (14)
C11—N2—C10	123.45 (14)	N2—C11—H11B	111.1 (14)
C2—C1—C6	120.75 (16)	C12—C11—H11B	112.3 (14)
C2—C1—S1	115.20 (13)	H11A—C11—H11B	108.8 (19)
C6—C1—S1	123.97 (13)	O2—C12—C11	105.47 (13)
C3—C2—C1	120.61 (17)	O2—C12—H12A	108.2 (14)
C3—C2—H2	122.4 (14)	C11—C12—H12A	110.6 (13)
C1—C2—H2	117.0 (14)	O2—C12—H12B	106.3 (14)
C2—C3—C4	119.33 (17)	C11—C12—H12B	112.9 (14)
C2—C3—H3	119.4 (15)	H12A—C12—H12B	113.0 (19)
C4—C3—H3	121.2 (15)	O3—C13—N2	128.64 (16)
C5—C4—C3	120.53 (17)	O3—C13—O2	122.07 (15)
C5—C4—H4	119.3 (14)	N2—C13—O2	109.30 (14)
C3—C4—H4	120.1 (14)	C8—C14—C15	131.80 (16)
C4—C5—C6	120.93 (16)	C8—C14—H14	113.7 (13)
C4—C5—H5	117.9 (14)	C15—C14—H14	114.5 (13)
C6—C5—H5	121.2 (14)	C16—C15—C20	115.34 (16)
C1—C6—C5	117.79 (15)	C16—C15—C14	125.33 (16)
C1—C6—N1	121.60 (15)	C20—C15—C14	119.31 (16)
C5—C6—N1	120.60 (15)	C17—C16—C15	122.84 (18)
O1—C7—N1	119.71 (15)	C17—C16—H16	114.8 (15)
O1—C7—C8	119.48 (15)	C15—C16—H16	122.4 (15)
N1—C7—C8	120.77 (14)	C18—C17—C16	118.95 (18)
C14—C8—C7	115.16 (15)	C18—C17—H17	118.7 (16)
C14—C8—S1	123.40 (13)	C16—C17—H17	122.4 (16)
C7—C8—S1	121.39 (12)	C17—C18—C19	121.36 (17)
N1—C9—C10	112.06 (14)	C17—C18—Cl1	119.91 (15)
N1—C9—H9A	109.0 (12)	C19—C18—Cl1	118.70 (15)
C10—C9—H9A	113.1 (12)	C20—C19—C18	118.45 (18)
N1—C9—H9B	106.8 (12)	C20—C19—H19	118.9 (13)
C10—C9—H9B	108.7 (12)	C18—C19—H19	122.7 (13)
H9A—C9—H9B	106.9 (16)	C19—C20—C15	123.05 (17)

N2—C10—C9	110.45 (14)	C19—C20—Cl2	116.31 (14)
N2—C10—H10A	110.7 (12)	C15—C20—Cl2	120.64 (13)
C8—S1—C1—C2	-175.06 (14)	C11—N2—C10—C9	81.1 (2)
C8—S1—C1—C6	8.14 (18)	N1—C9—C10—N2	-175.21 (14)
C6—C1—C2—C3	0.3 (3)	C13—N2—C11—C12	-8.6 (2)
S1—C1—C2—C3	-176.63 (16)	C10—N2—C11—C12	173.17 (16)
C1—C2—C3—C4	-1.5 (3)	C13—O2—C12—C11	-10.95 (19)
C2—C3—C4—C5	0.6 (3)	N2—C11—C12—O2	11.27 (19)
C3—C4—C5—C6	1.5 (3)	C11—N2—C13—O3	-177.18 (18)
C2—C1—C6—C5	1.8 (3)	C10—N2—C13—O3	1.1 (3)
S1—C1—C6—C5	178.44 (13)	C11—N2—C13—O2	2.2 (2)
C2—C1—C6—N1	-177.45 (16)	C10—N2—C13—O2	-179.56 (15)
S1—C1—C6—N1	-0.8 (2)	C12—O2—C13—O3	-174.76 (16)
C4—C5—C6—C1	-2.7 (3)	C12—O2—C13—N2	5.81 (18)
C4—C5—C6—N1	176.56 (16)	C7—C8—C14—C15	-176.93 (18)
C7—N1—C6—C1	-9.1 (3)	S1—C8—C14—C15	0.3 (3)
C9—N1—C6—C1	172.24 (16)	C8—C14—C15—C16	6.6 (3)
C7—N1—C6—C5	171.68 (17)	C8—C14—C15—C20	-175.08 (19)
C9—N1—C6—C5	-7.0 (2)	C20—C15—C16—C17	0.6 (3)
C6—N1—C7—O1	-173.69 (16)	C14—C15—C16—C17	179.02 (19)
C9—N1—C7—O1	5.0 (2)	C15—C16—C17—C18	-0.3 (3)
C6—N1—C7—C8	8.7 (3)	C16—C17—C18—C19	0.1 (3)
C9—N1—C7—C8	-172.58 (15)	C16—C17—C18—Cl1	-178.22 (16)
O1—C7—C8—C14	0.9 (3)	C17—C18—C19—C20	-0.3 (3)
N1—C7—C8—C14	178.52 (16)	Cl1—C18—C19—C20	178.04 (15)
O1—C7—C8—S1	-176.37 (14)	C18—C19—C20—C15	0.7 (3)
N1—C7—C8—S1	1.2 (2)	C18—C19—C20—Cl2	-178.85 (15)
C1—S1—C8—C14	174.78 (16)	C16—C15—C20—C19	-0.8 (3)
C1—S1—C8—C7	-8.17 (17)	C14—C15—C20—C19	-179.34 (18)
C7—N1—C9—C10	-88.22 (19)	C16—C15—C20—Cl2	178.68 (14)
C6—N1—C9—C10	90.61 (19)	C14—C15—C20—Cl2	0.2 (2)
C13—N2—C10—C9	-97.0 (2)		

Symmetry codes: (i) $-x, y+1/2, -z+3/2$; (ii) $-x+1, y+1/2, -z+1/2$; (iii) $x, y+1, z$; (iv) $-x, -y+1, -z+1$; (v) $-x+1, -y+1, -z+1$; (vi) $-x+1, -y+1, -z$.